

# ACT-CONSISTENT $B - L$ HIGGS INFLATION IN SUPERGRAVITY

---

**C. PALLIS**

*School of Technology,*

*Aristotle University of Thessaloniki,*

*Thessaloniki, GR-541 24 GREECE*

*E-mail: kpallis@auth.gr*

**ABSTRACT:** We consider a renormalizable extension of the minimal supersymmetric standard model (MSSM) endowed by an R and a gauged  $B - L$  symmetry. The model incorporates chaotic inflation driven by a quartic potential, associated with the Higgs superfields which lead to a spontaneous breaking of  $U(1)_{B-L}$ . Consistency with the ACT data is achieved by considering a fractional shift-symmetric Kähler potential which includes two free parameters ( $p, N$ ) constrained in the ranges  $1.355 \leq p \leq 6.7$  and  $6 \cdot 10^{-5} \leq N \leq 0.7$ . An explanation of the  $\mu$  term of the MSSM is also provided, under the condition that a related parameter in the superpotential is somewhat small. Baryogenesis occurs via non-thermal leptogenesis which is also realized by the inflaton's decay to the lightest and/or next-to-lightest right-handed neutrinos for normal ordered light neutrino masses.

**Published in** PoS CORFU 2025, 139 (2026).

---

*Corfu Summer Institute 2025 "School and Workshops on Elementary Particle Physics and Gravity"  
(CORFU2025) 24 August - 3 September, 2025  
Corfu, Greece*

## 1. INTRODUCTION

We focus on a variant of T-model inflation [1–3] called  $T_p$ -model *inflation* [4] which employs as inflaton the radial component of the Higgs superfields associated with a  $B - L$  phase transition. For this reason we call our model  $T_p$ -model *Higgs inflation* (HI) or for short pHl [5]. We embed it in a complete particle framework presented in Sec. 2. The inflationary part of this context is described in Sec. 3. Then, in Sec. 4, we explain how the  $\mu$  term of the *minimal supersymmetric standard model* (MSSM) is obtained and we outline how the observed *baryon asymmetry of the universe* (BAU) is generated via *non-thermal leptogenesis* (nTL). Our conclusions are summarized in Sec. 5. Throughout the text, the subscript of type  $,z$  denotes derivation *with respect to* (w.r.t) the field  $z$  and charge conjugation is denoted by a star. Unless otherwise stated, we use units where  $m_P = 2.43 \cdot 10^{18}$  GeV is taken unity.

## 2. MODEL DESCRIPTION

We focus on an elementary *Grand Unified Theory* (GUT) based on the gauge group

$$\mathbb{G}_{B-L} = \mathbb{G}_{\text{SM}} \times U(1)_{B-L} \quad \text{with} \quad \mathbb{G}_{\text{SM}} = SU(3)_C \times SU(2)_L \times U(1)_Y$$

being the gauge group of the standard model and  $B$  and  $L$  denoting the baryon and lepton number respectively. The model disposes also three global  $U(1)$  symmetries from which the  $U(1)_R$  symmetry plays a crucial role in our construction. The particle content of the model is shown in Table 1. The  $i$ th generation  $SU(2)_L$  doublet left-handed quark and lepton superfields are denoted by  $Q_i$  and  $L_i$  respectively, whereas the  $SU(2)_L$  singlet antiquark [antilepton] superfields by  $u_i^c$  and  $d_i^c$  [ $e_i^c$  and  $N_i^c$ ] respectively. The electroweak Higgs superfields which couple to the up [down] quark superfields are denoted by  $H_u$  [ $H_d$ ]. The breaking of  $U(1)_{B-L}$  is implemented by the Higgs superfields  $\bar{\Phi}$  and  $\Phi$ , which contain the inflaton too, whereas  $S$  is named stabilizer and plays an auxiliary role.

In Sec. 2.1 and 2.1 below we specify the building blocks of our model.

### 2.1 SUPERPOTENTIAL

The superpotential of our model naturally splits into two parts:

$$W = W_{\text{MSSM}} + W_{\text{B}}, \quad \text{where} \quad (2.1)$$

(a)  $W_{\text{MSSM}}$  is the part of  $W$  which contains the usual terms – except for the  $\mu$  term – of MSSM, supplemented by the last term which provides Dirac masses to neutrinos

$$W_{\text{MSSM}} = h_{ijD} d_i^c Q_j H_d + h_{ijU} u_i^c Q_j H_u + h_{ijE} e_i^c L_j H_d + h_{ijN} N_i^c L_j H_u. \quad (2.2a)$$

(b)  $W_{\text{B}}$  is the part of  $W$  (“B”eyond that of MSSM) which is relevant for pHl, the generation of the  $\mu$  term of MSSM and the Majorana masses for neutrinos. It takes the form

$$W_{\text{B}} = \lambda S (\bar{\Phi}\Phi - M^2/2) + \lambda_{\mu} S H_u H_d + \lambda_{iN^c} \bar{\Phi} N_i^{c2}. \quad (2.2b)$$

The imposed  $U(1)_R$  symmetry ensures the linearity of  $W_{\text{B}}$  w.r.t  $S$ . The first two terms support the implementation of pHl. The third term plays a key role in the resolution of the  $\mu$  problem of MSSM. The fourth term in Eq. (2.2b) provides the Majorana masses for the  $N_i^c$ 's and assures the decay of the inflaton to  $\tilde{N}_i^c$ , whose subsequent decay can activate nTL – see Sec. 4.2.

SUPERFIELDS	REPRESENTATIONS UNDER $\mathbb{G}_{B-L}$	GLOBAL SYMMETRIES		
		$R$	$B$	$L$
MATTER FIELDS				
$e_i^c$	$(\mathbf{1}, \mathbf{1}, 1, 1)$	1	0	-1
$N_i^c$	$(\mathbf{1}, \mathbf{1}, 0, 1)$	1	0	-1
$L_i$	$(\mathbf{1}, \mathbf{2}, -1/2, -1)$	1	0	1
$u_i^c$	$(\mathbf{3}, \mathbf{1}, -2/3, -1/3)$	1	-1/3	0
$d_i^c$	$(\mathbf{3}, \mathbf{1}, 1/3, -1/3)$	1	-1/3	0
$Q_i$	$(\mathbf{\bar{3}}, \mathbf{2}, 1/6, 1/3)$	1	1/3	0
HIGGS FIELDS				
$H_d$	$(\mathbf{1}, \mathbf{2}, -1/2, 0)$	0	0	0
$H_u$	$(\mathbf{1}, \mathbf{2}, 1/2, 0)$	0	0	0
$S$	$(\mathbf{1}, \mathbf{1}, 0, 0)$	2	0	0
$\Phi$	$(\mathbf{1}, \mathbf{1}, 0, 2)$	0	0	-2
$\bar{\Phi}$	$(\mathbf{1}, \mathbf{1}, 0, -2)$	0	0	2

TABLE 1: Representations under  $\mathbb{G}_{B-L}$  and the extra global charges of the superfields of our model.

## 2.2 KÄHLER POTENTIAL

pHI is feasible if  $W_B$  cooperates [5] with the following Kähler potential

$$K = \tilde{K}_I(\bar{\Phi}, \Phi) + K_{\text{st}}(X^\alpha), \quad (2.3)$$

which includes two contributions: the first one is devoted to  $\bar{\Phi} - \Phi$  system and the second one to  $X^\alpha = S, H_u, H_d, \tilde{N}_i^c, \tilde{L}_i$ . In particular,

$$K_{\text{st}} = N_{\text{st}} \ln(1 + |X^\alpha|^2/N_{\text{st}}), \quad (2.4a)$$

where  $0 < N_{\text{st}} < 6$  and the complex scalar components of the Higgs superfields are denoted by the same superfield symbol whereas these of  $N_i^c$  and  $L_i$  by  $\tilde{N}_i^c$  and  $\tilde{L}_i$  respectively.  $K_{\text{st}}$  parameterizes the compact Kähler manifold  $SU(15)/U(1)$  with constant scalar curvature  $14 \cdot 15/N_{\text{st}} = 210/N_{\text{st}}$  [11] and successfully stabilizes  $X^\alpha$  along the inflationary path – see below – without invoking higher order terms. On the other hand,  $\tilde{K}_I$  includes two terms

$$\tilde{K}_I = K_I + K_{\text{sh}}, \quad (2.4b)$$

from which  $K_I$  is real and fractional – for an alternative choice see Ref. [5] – whereas  $K_{\text{sh}}$  includes an holomorphic (and an anti-holomorphic) part rendering  $\tilde{K}_I$  shift-symmetric. Namely,

$$K_I = \frac{N}{(1 - |\Phi|^2 - |\bar{\Phi}|^2)^p} \quad \text{and} \quad K_{\text{sh}} = -\frac{N}{2} \frac{(1 - 2\bar{\Phi}\Phi)^p + (1 - 2\bar{\Phi}^*\Phi^*)^p}{(1 - 2\bar{\Phi}\Phi)^p (1 - 2\bar{\Phi}^*\Phi^*)^p}. \quad (2.4c)$$

They are defined for  $N > 0$ ,  $\bar{\Phi}\Phi < 1/2$  and  $|\Phi|^2 + |\bar{\Phi}|^2 < 1$ .  $\tilde{K}_I$  is invariant under  $\mathbb{G}_{B-L}$  and the interchange  $\Phi \leftrightarrow \bar{\Phi}$  and introduces two free parameters  $(p, N)$ . It parameterizes hyperbolic Kähler manifold but without constant curvature, unlike the case of T-model HI [2, 3].

### 3. INFLATIONARY SCENARIO

The salient features of our inflationary scenario are studied at tree level in Sec. 3.1 and at one-loop level in Sec. 3.2. We then present its predictions in Sec. 3.4, calculating a number of observable quantities introduced in Sec. 3.3.

#### 3.1 INFLATIONARY POTENTIAL

We express  $\Phi, \bar{\Phi}$  and  $X^\alpha = S, H_u, H_d, \tilde{N}_i^c, \tilde{L}_i$  according to the parametrization

$$\Phi = \phi e^{i\theta} \cos \theta_\Phi, \quad \bar{\Phi} = \phi e^{i\bar{\theta}} \sin \theta_\Phi \quad \text{and} \quad X^\alpha = (x^\alpha + i\bar{x}^\alpha)/\sqrt{2}, \quad (3.1)$$

where  $0 \leq \theta_\Phi \leq \pi/2$ . We then find the SUGRA scalar potential  $V$  via the formula

$$V = V_F + V_D \quad \text{with} \quad V_F = e^K \left( K^{\alpha\bar{\beta}} D_\alpha W_B D_{\bar{\beta}}^* W_B^* - 3|W_B|^2 \right) \quad \text{and} \quad V_D = \frac{1}{2} g^2 D_{B-L}^2, \quad (3.2)$$

where  $K_{\alpha\bar{\beta}} = K_{,Z^\alpha Z^{*\bar{\beta}}}$ ,  $K^{\alpha\bar{\beta}} K_{\alpha\bar{\gamma}} = \delta_{\bar{\gamma}}^{\bar{\beta}}$ ,  $D_\alpha W = W_{,Z^\alpha} + K_{,Z^\alpha} W$  and  $D_{B-L} = Z_\alpha (B - L) K^\alpha$ . Also  $g$  is the gauge coupling constant (considered unified),  $D_{B-L}$  takes the form

$$D_{B-L} = Np (|\Phi| - |\bar{\Phi}|) / 2 (1 - |\Phi|^2 - |\bar{\Phi}|^2)^{p+1} \quad (3.3)$$

(for  $\tilde{N}_i^c = \tilde{L}_i = 0$ ) and suggests that the inflaton can be identified with the component  $\phi$  in Eq. (3.1) which assures  $|\Phi| = |\bar{\Phi}|$ . Therefore,  $p$ HI can take place along the D-flat direction

$$\langle x^\alpha \rangle_I = \langle \bar{x}^\alpha \rangle_I = \langle \theta \rangle_I = \langle \bar{\theta} \rangle_I = 0 \quad \text{and} \quad \langle \theta_\Phi \rangle_I = \pi/4, \quad (3.4)$$

where the symbol  $\langle Q \rangle_I$  represents values of  $Q$  during  $p$ HI. The inflationary potential  $V_{p\text{HI}}$  can be derived as follows

$$V_{p\text{HI}} = \langle V \rangle_I = \langle e^K K^{SS^*} \rangle_I |W_{B,S}|^2 = \lambda^2 (\phi^2 - M^2)^2 / 4. \quad (3.5)$$

To determine the canonically normalized fields, we note that  $\langle K_{\alpha\bar{\beta}} \rangle_I$  takes the form

$$\langle K_{\alpha\bar{\beta}} \rangle_I = \text{diag} \left( \langle M_{\bar{\Phi}\Phi} \rangle_I, \underbrace{1, \dots, 1}_{14 \text{ elements}} \right) \quad \text{with} \quad \langle M_{\bar{\Phi}\Phi} \rangle_I = \frac{pN}{f_T^{2+p}} \begin{pmatrix} \kappa & \bar{\kappa} \\ \bar{\kappa} & \kappa \end{pmatrix} \quad \text{and} \quad K_{X^\alpha X^{*\bar{\alpha}}} = 1. \quad (3.6)$$

Here  $\kappa = f_T + fp$ , with  $f_T = 1 - \phi^2$  and  $f_p = 1 + p\phi^2$ , and  $\bar{\kappa} = (1+p)\phi^2$ . Upon diagonalization of  $\langle M_{\bar{\Phi}\Phi} \rangle_I$  we find its eigenvalues which are

$$\kappa_+ = \kappa = pN f_p / f_T^{p+2} \quad \text{and} \quad \kappa_- = pN / f_T^{p+1}. \quad (3.7)$$

Inserting Eqs. (3.1) and (3.6) into the kinetic term of the SUGRA action,  $K_{\alpha\bar{\beta}} \dot{Z}^\alpha \dot{Z}^{\bar{\beta}}$ , we can specify the canonically normalized fields, denoted by hat, as follows

$$\frac{d\hat{\phi}}{d\phi} = J, \quad \hat{\theta}_\pm = \sqrt{\kappa_\pm} \phi \theta_\pm, \quad \hat{\theta}_\Phi = \sqrt{2\kappa_-} \phi \left( \theta_\Phi - \frac{\pi}{4} \right) \quad \text{and} \quad (\hat{x}^\alpha, \hat{\bar{x}}^\alpha) = (x^\alpha, \bar{x}^\alpha), \quad (3.8)$$

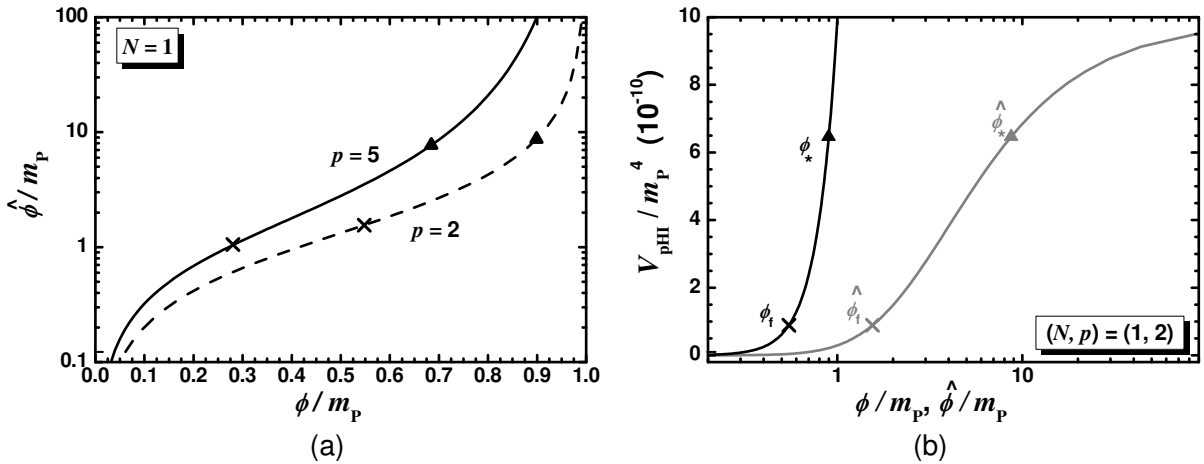


**FIGURE 1:** (a) Canonically normalized inflaton  $\hat{\phi}$  as a function of  $\phi$  for  $N = 1$  and  $p = 5$  (solid line) or  $p = 2$  (dashed line); (b) inflationary potential  $V_{\text{pHI}}$  for  $(p, N) = (1, 2)$  as a function of  $\phi$  (black line) and  $\hat{\phi}$  (gray line). Values corresponding to  $\phi_*$ ,  $\phi_f$ ,  $\hat{\phi}_*$  and  $\hat{\phi}_f$  are also depicted in both panels.

where  $J = \sqrt{2\kappa_+}$  and  $\theta_{\pm} = (\bar{\theta} \pm \theta)/\sqrt{2}$ . As we show below, the masses of the scalars besides  $\hat{\phi}$  during pHI are heavy enough such that the dependence of the hatted fields on  $\phi$  does not influence their dynamics.

Taking into account the results in Eqs. (3.5) and (3.8) we depict  $\hat{\phi}$  as a function of  $\phi$  for  $N = 1$  and  $p = 5$  (solid line) or  $p = 2$  (dashed line) in Fig. 1-(a) and  $V_{\text{pHI}}$  for  $(p, N) = (2, 1)$  as a function of  $\phi$  (black line) and  $\hat{\phi}$  (gray line) in Fig. 1-(a). From the former plot, we can remark that  $\hat{\phi}$  increases w.r.t  $\phi$  rendering pHI possible even for  $\phi < 1$ , whereas from the latter we see that  $V_{\text{pHI}}$  as a function of  $\phi$  has the well-known parabolic-like slope but as a function of  $\hat{\phi}$  experiences a stretching for  $\hat{\phi} > 1$  rendering it suitable for pHI – cf. Ref. [1, 2, 4].

### 3.2 STABILITY AND ONE-LOOP RADIATIVE CORRECTIONS

We here demonstrate that the inflationary direction in Eq. (3.4) is stable w.r.t the fluctuations of the non-inflaton fields. To this end, we construct the mass-squared spectrum of the scalars taking into account the canonical normalization of the various fields in Eq. (3.8). We find the expressions of the masses squared  $\hat{m}_{z^\alpha}^2$  (with  $z^\alpha = \theta_+, \theta_\Phi, x^\alpha$  and  $\bar{x}^\alpha$ ) arranged in Table 2. The various unspecified there eigenstates are defined as follows

$$h_{\pm} = (h_u \pm h_d)/\sqrt{2}, \quad \hat{h}_{\pm} = (\hat{h}_u \pm \hat{h}_d)/\sqrt{2} \quad \text{and} \quad \hat{\psi}_{\pm} = (\hat{\psi}_{\Phi_+} \pm \hat{\psi}_S)/\sqrt{2}, \quad (3.9a)$$

where the (unhatted) spinors  $\psi_\Phi$  and  $\psi_{\bar{\Phi}}$  associated with the superfields  $\Phi$  and  $\bar{\Phi}$  are related to the normalized (hatted) ones in Table 2 as follows

$$\hat{\psi}_{\Phi_{\pm}} = \sqrt{\kappa_{\pm}} \psi_{\Phi_{\pm}} \quad \text{with} \quad \psi_{\Phi_{\pm}} = (\psi_\Phi \pm \psi_{\bar{\Phi}})/\sqrt{2}. \quad (3.9b)$$

From Table 2 it is evident that  $0 < N_X \leq 6$  assists us to achieve  $m_s^2 > H_{\text{pHI}}^2 = V_{\text{pHI}}/3$  – in accordance with the results of Ref. [11] – and also enhances the ratios  $m_{X^\gamma}^2/H_{\text{pHI}}^2$  for  $X^\gamma = H_u, H_d, \tilde{N}_i^c, \tilde{L}_i$  w.r.t the values that we would have obtained, if we had used just canonical terms in  $K_{\text{st}}$  – see Eq. (2.4a). On the other hand,  $m_{h_-}^2 > 0$  requires

$$\lambda_\mu < \lambda(1 + N_{\text{st}})\phi_f^2/2N_{\text{st}}, \quad (3.10)$$

FIELDS	EIGENSTATES	MASSES SQUARED	
30 real scalars	$\widehat{\theta}_+$	$m_{\theta_+}^2$	$6H_{\text{pHI}}^2$
	$\widehat{\theta}_\Phi$	$m_{\theta_\Phi}^2$	$M_{BL}^2 + 6H_{\text{pHI}}^2$
	$s, \bar{s}$	$m_s^2$	$6H_{\text{pHI}}^2 \left(1/N_{\text{st}} + 2f_{\text{T}}^{p+2}/pN\phi^2 f_p\right)$
	$h_\pm, \bar{h}_\pm$	$m_{h_\pm}^2$	$3H_{\text{pHI}}^2 (1 + 1/N_{\text{st}} \pm 2\lambda_\mu/\lambda\phi^2)$
	$\tilde{\nu}_i^c, \bar{\tilde{\nu}}_i^c$	$m_{\tilde{\nu}^c}^2$	$3H_{\text{pHI}}^2 (1 + 1/N_{\text{st}} + 8\lambda_{iN^c}^2/\lambda^2\phi^2)$
	$\tilde{l}_i, \bar{\tilde{l}}_i$	$m_{\tilde{l}}^2$	$3H_{\text{pHI}}^2 (1 + 1/N_{\text{st}})$
1 gauge boson	$A_{BL}$	$M_{BL}^2$	$2g^2 N p \phi^2 / f_{\text{T}}^{p+1}$
7 Weyl spinors	$\widehat{\psi}_\pm$	$m_{\psi_\pm}^2$	$6H_{\text{pHI}}^2 f_{\text{T}}^{p+2} / pN\phi^2 f_p$
	$N_i^c$	$M_{iN^c}^2$	$24H_{\text{pHI}}^2 \lambda_{iN^c}^2 / \lambda^2 \phi^2$
	$\lambda_{BL}, \widehat{\psi}_{\Phi-}$	$M_{BL}^2$	$2g^2 N p \phi^2 / f_{\text{T}}^{p+1}$

**TABLE 2:** The mass squared spectrum of our models along the path in Eq. (3.4).

where  $\phi_f$  is the  $\phi$  value at the end of pHI – see Sec. 3.3 below. The upper bound above numerically equals to  $2 \cdot 10^{-5}$  for  $N_{\text{st}} = 1$ . Despite its low value,  $\lambda_\mu$  can become compatible with  $\mu/m_{3/2} \sim 1$  as we show in Sec. 4.1 – here  $m_{3/2}$  is the  $\tilde{G}$  mass. In Table 2 we display also the mass  $M_{BL}$  of the gauge boson which becomes massive having ‘eaten’ the Goldstone boson  $\theta_-$ . This signals the fact that  $\mathbb{G}_{B-L}$  is broken during pHI and so no cosmological defects (cosmic strings in our case) are produced.

The derived mass spectrum can be employed in order to find the one-loop radiative corrections  $\Delta V_{\text{pHI}}$  to  $V_{\text{pHI}}$ . Considering SUGRA as an effective theory with cutoff scale equal to  $m_{\text{P}}$ , the well-known Coleman-Weinberg formula can be employed self-consistently taking into account only the masses which lie well below the UV cut-off scale  $m_{\text{P}}$ , i.e., all the masses arranged in Table 2 besides  $M_{BL}$  and  $m_{\theta_\Phi}$  – cf. Ref. [5, 9, 12]. The resulting  $\Delta V_{\text{pHI}}$  takes the form

$$\Delta V_{\text{pHI}} = \frac{1}{64\pi^2} \sum_{\alpha} N_{\alpha} m_{\alpha}^4 \ln \frac{m_{\alpha}^2}{\Lambda_{\text{CW}}^2} - 6M_{iN^c}^4 \ln \frac{M_{iN^c}^2}{\Lambda_{\text{CW}}^2} \quad \text{where} \quad \begin{cases} \alpha & = \{\theta_+, s, h_{\pm}, i\tilde{\nu}^c, \tilde{l}, \psi_{\Phi\pm}\} \\ N_{\alpha} & = \{1, 2, 8, 6, 12, -4\} \end{cases} \quad (3.11)$$

and lets intact our inflationary outputs, provided that the renormalization-group mass scale  $\Lambda_{\text{CW}}$ , is determined by requiring  $\Delta V_{\text{pHI}}(\phi_*) = 0$  or  $\Delta V_{\text{pHI}}(\phi_f) = 0$  – see below.

### 3.3 INFLATIONARY OBSERVABLES

A period of slow-roll pHI is controlled by the strength of the slow-roll parameters

$$\epsilon = \left( \frac{V_{\text{pHI}, \widehat{\phi}}}{\sqrt{2}V_{\text{pHI}}} \right)^2 \simeq \frac{4f_{\text{T}}^{p+2}}{pNf_p\phi^2} \quad \text{and} \quad \eta = \frac{V_{\text{pHI}, \widehat{\phi\phi}}}{V_{\text{pHI}}} \simeq 2f_{\text{T}}^{p+1} \frac{3 + (p-5)\phi^2 - p(p+4)\phi^4}{pN\phi^2 f_p^2}. \quad (3.12)$$

Expanding  $\epsilon$  and  $\eta$  for  $\phi \ll 1$  we can find that pHI terminates for  $\phi = \phi_f$  such that

$$\max\{\epsilon(\phi_f), |\eta(\phi_f)|\} = 1 \quad \Rightarrow \quad \phi_f \simeq \sqrt{6/(16 + 3Np)}, \quad (3.13)$$

which increases as  $N$  decreases and so pHI can be established easier for relatively large  $N$ 's.

The number of e-foldings,  $N_*$ , that the pivot scale  $k_* = 0.05/\text{Mpc}$  suffers during pHI can be calculated through the relation

$$N_* = \int_{\hat{\phi}_f}^{\hat{\phi}_*} d\hat{\phi} \frac{V_{\text{pHI}}}{V_{\text{pHI},\hat{\phi}}} \simeq \frac{pN\phi_*^2}{4f_{\text{T}*}^{1+p}} \Rightarrow \phi_* \simeq \sqrt{1 - \left(\frac{pN}{4N_*}\right)^{1/(p+1)}}, \quad (3.14)$$

where  $\hat{\phi}_* [\phi_*]$  is the value of  $\hat{\phi} [\phi]$  when  $k_*$  crosses the inflationary horizon and we take into account that  $\phi_f \ll \phi_*$ . Apparently,  $\phi_* < 1$  and so our proposal can be stabilized against corrections from higher order terms of the form  $(\bar{\Phi}\Phi)^\ell$  with  $\ell > 1$  in  $W_B$  – see Eq. (2.2b).

The amplitude  $A_s$  of the power spectrum of the curvature perturbations generated by  $\phi$  at the pivot scale  $k_*$  is estimated as follows

$$\sqrt{A_s} = \frac{1}{2\sqrt{3}\pi} \frac{V_{\text{pHI}}(\hat{\phi}_*)^{3/2}}{|V_{\text{pHI},\hat{\phi}}(\hat{\phi}_*)|} \Rightarrow \lambda \simeq 2^{(n/4+5/2)} \sqrt{3A_s} \pi f_{\text{T}*}^{p/2+1} / \phi_*^3 \sqrt{pN f_{p*}}. \quad (3.15)$$

The resulting relation yields numerically  $\lambda \sim 10^{-6}$ .

At the pivot scale we can also calculate the scalar spectral index  $n_s$ , its running  $a_s$ , and the tensor-to-scalar ratio  $r$  via the relations

$$n_s = 1 - 6\epsilon_* + 2\eta_* \simeq 1 - \frac{p+2}{(p+1)N_*}, \quad r = 16\epsilon_* \simeq \frac{4(4^p p N)^{1/(p+1)}}{(p+1)N_*^{(p+2)/(p+1)}}, \quad (3.16a)$$

$$a_s = \frac{2}{3} (4\eta_*^2 - (n_s - 1)^2) - 2\xi_* \simeq -\frac{p+2}{(p+1)N_*^2} \quad \text{with} \quad \xi = V_{\text{pHI},\hat{\phi}} V_{\text{pHI},\hat{\phi}\hat{\phi}} / V_{\text{pHI}}^2. \quad (3.16b)$$

Here the variables with subscript  $*$  are evaluated at  $\phi = \phi_*$ . A clear dependence of the observables on  $p$  arises which renders our results friendly to ACT as it is evident for  $p = 1$  or 2 and  $N_* = 55$ . Note also that the expressions above for  $n_s$  and  $a_s$  are independent from  $N$ . This fact, however, is not totally kept as we show numerically below.

### 3.4 COMPARISON WITH OBSERVATIONS

The approximate analytic expressions above can be verified by the numerical analysis of our model. Namely, we apply the accurate expressions in Eqs. (3.14) and (3.15) and confront the corresponding observables with the requirements [7]

$$N_* \simeq 61.5 + \ln \left( V_{\text{pHI}}(\phi_*)^{1/2} / V_{\text{pHI}}(\phi_f)^{1/4} \right) \quad \text{and} \quad A_s^{1/2} \simeq 4.618 \cdot 10^{-5}, \quad (3.17)$$

where we consider in the left-hand side relation an equation-of-state parameter  $w_{\text{rh}} \simeq 1/3$  corresponding to quartic potential which approximates [5] rather well  $V_{\text{pHI}}$  for  $\phi \ll 1$ . The constraints above allows us to extract  $\lambda$  and  $\phi_*$  for any given  $p$ ,  $N$  and  $M$ . However, if  $M \ll m_{\text{P}}$  then  $M$  is irrelevant for the inflationary observables. Motivated by the unification of the gauge coupling constants within MSSM, we determine  $M$  doing the identification

$$\langle M_{BL} \rangle = M_{\text{G}} \Rightarrow M \simeq M_{\text{G}} / g \sqrt{2Np}, \quad (3.18)$$

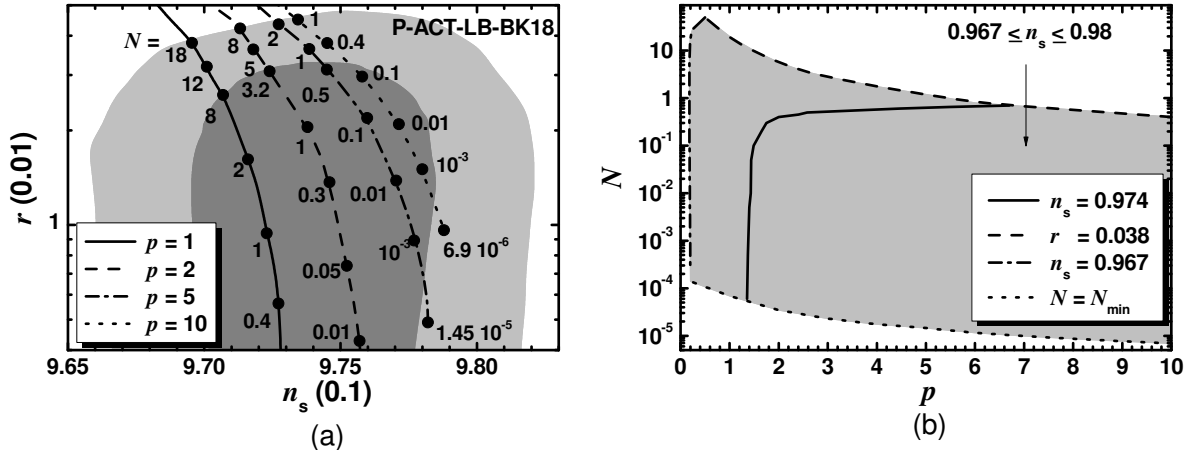


**FIGURE 2:** (a) Allowed curves in the  $n_s - r$  plane with the  $N$  values indicated along them – the marginalized joint 68% [95%] region from P-ACT-LB-BK18 data is depicted by the dark [light] shaded contour; (b) Allowed (shaded) region as determined by Eq. (3.17) – (3.20) in the  $p - N$  plane. The conventions adopted for the various lines are also shown in both panels.

where we take into account that  $\langle f_T \rangle \simeq 1$  and  $\langle \phi \rangle = M$  in accordance with Eq. (4.3) – see below. We use the numerical values  $g \simeq 0.7$  for the value of the GUT gauge coupling constant and  $M_G \simeq 2/2.433 \cdot 10^{-2}$  for the unification scale. The success of our inflationary setting is assured if we impose a lower bound on  $N$  derived as follows

$$M \lesssim m_P \Rightarrow N \gtrsim N_{\min} = M_G^2 / 2g^2 p m_P^2. \quad (3.19)$$

Given Eq. (3.18), our final set of free input parameters is  $(p, N)$  and it can be constrained by comparing our results on  $n_s$  and  $r$ , computed via the definitive relations in Eq. (3.16a), against the combination of the ACT DR6 with the measurements from other experiments [7]. The so-obtained P-ACT-LB-BK18 data suggests

$$n_s = 0.9743 \pm 0.0068 \text{ and } r \leq 0.038, \quad (3.20)$$

at 95% confidence level (c.l.) with  $|a_s| \ll 0.01$  – ramifications of the restrictions above for several inflationary models are recently reviewed in Ref. [8]. More precisely, in Fig. 2-(a), we place over the top of the allowed contours of the P-ACT-LB-BK18 data in the  $n_s - r$  plane the lines predicted by our model after imposing Eqs. (3.17), (3.18) and (3.19). We draw solid, dashed, dot-dashed and dotted lines for  $p = 1, 2, 5$  and  $10$  respectively and show the variation of  $N$  along each line. For the two latter  $p$ 's the corresponding  $N_{\min}$  values from Eq. (3.19) are also displayed. We clearly see that  $n_s$  increases with  $p$  and  $r$  with  $N$  and so the whole shaded region favored by P-ACT-LB-BK18 is covered varying  $p$  and  $N$ . As a bonus, the resulting  $r$ 's for  $(p, N)$ 's of order unity are also testable by the forthcoming experiments [10], like BICEP3, PRISM and LiteBIRD, searching for primordial gravity waves since  $r \gtrsim 0.007$ .

The variation of the observables in Fig. 2-(a) reveals that our free parameters can be constrained in the  $p - N$  plane. The relevant allowed region is shown in Fig. 2-(b) with boundary curves originated from (i) the bound on  $r$  in Eq. (3.20) (dashed line), (ii) the lower bound on

$n_s$  in Eq. (3.20) (dot-dashed line) and (iii) the lower bound on  $N$  in Eq. (3.19) (dotted line) – we take by hand a maximal  $p = 10$  since no upper bound on  $p$  can be inferred from the corresponding bound on  $n_s$  in Eq. (3.20). Fixing  $n_s$  to its central value in Eq. (3.20), we obtain the solid line along which we obtain

$$1.355 \lesssim p \lesssim 6.7 \quad \text{and} \quad 6 \cdot 10^{-5} \lesssim N \lesssim 0.7 \quad (3.21)$$

with  $N_\star \simeq (54.7 - 56.8)$ ,  $a_s \simeq -4.7 \cdot 10^{-4}$  and  $r \gtrsim 2.8 \cdot 10^{-4}$ . The obtained  $|a_s|$ 's remain negligibly small being, thereby, consistent with its 95% c.l. allowed margin in Ref. [7]. The closer to unity  $\phi_\star$  is chosen, the largest  $N_\star$  is obtained. To quantify the relevant tuning we estimate  $\Delta_\star = 1 - \phi_\star$  which ranges in the interval (0.8 – 28)% for the values in Eq. (3.21). The maximal  $\Delta_\star$  values are obtained for the largest  $p$ 's and  $N$ 's indicating, thereby that naturalness prefers  $N$  and  $p$  values of order unity.

Note, finally, that the one loop radiative corrections in Eq. (3.11) let immune our results provided we impose one of the two conditions mentioned below the aforementioned equation. E.g., imposing the first of them for  $N_{\text{st}} = 1$  and  $p = 2$  we find  $\Lambda_{\text{CW}} \simeq (4 - 5)$  YeV – hereafter we restore units, i.e., we take  $m_{\text{P}} = 2.43 \cdot 10^{18}$  GeV. Under these circumstances, our inflationary predictions can be exclusively reproduced by using  $V_{\text{pHI}}$  in Eq. (3.5).

## 4. POST-INFLATIONARY SCENARIO

Two byproducts of our setting is the derivation of the  $\mu$  term of MSSM, as shown in Sec. 4.1, and the implementation of baryogenesis via nTL as described in Sec. 4.2.

### 4.1 GENERATION OF THE $\mu$ TERM OF MSSM

The origin of the  $\mu$  term of MSSM can be explained if we combine the three first terms of Eq. (2.2b) working at the level of SUSY. In fact, the total low energy potential is

$$V_{\text{tot}} = V_{\text{SUSY}} + V_{\text{soft}}, \quad (4.1)$$

where the first term includes the SUSY limit  $V_{\text{SUSY}}$  of  $V_{\text{pHI}}$  in Eq. (3.5) which is given by

$$V_{\text{SUSY}} = K_{\text{SUSY}}^{\alpha\bar{\beta}} W_{\text{B}\alpha} W_{\text{B}\bar{\beta}}^*. \quad (4.2a)$$

Here  $K_{\text{SUSY}}$  is the limit of the  $K$  Eq. (2.3) for  $m_{\text{P}} \rightarrow \infty$ , which is

$$K_{\text{SUSY}} = Np (|\Phi|^2 + |\bar{\Phi}|^2 - \bar{\Phi}\Phi - \bar{\Phi}^*\Phi^*) + |X^\alpha|^2. \quad (4.2b)$$

Upon substitution of  $K_{\text{SUSY}}$  into Eq. (4.2a) we obtain

$$V_{\text{SUSY}} = \lambda^2 |\bar{\Phi}\Phi - M^2/2|^2 + \lambda^2 |S|^2 (|\bar{\Phi}|^2 + |\Phi|^2) / Np + \dots,$$

where the ellipsis includes terms which vanish at the SUSY vacuum lying along the D-flat direction  $|\bar{\Phi}| = |\Phi|$  with

$$\langle X^\alpha \rangle = 0 \quad \text{and} \quad |\langle \Phi \rangle| = |\langle \bar{\Phi} \rangle| = M/\sqrt{2}. \quad (4.3)$$

As a consequence,  $\langle \Phi \rangle$  and  $\langle \bar{\Phi} \rangle$  break spontaneously  $U(1)_{B-L}$  down to  $\mathbb{Z}_2^{B-L}$ . Since  $U(1)_{B-L}$  is already broken during pHI, no cosmic strings are formed.

The contributions from the soft SUSY-breaking terms, although negligible during pHI, since these are much smaller than  $\phi$ , may shift slightly  $\langle S \rangle$  from zero in Eq. (4.3). Indeed, the relevant potential terms are

$$V_{\text{soft}} = \left( \lambda A_\lambda S \bar{\Phi} \Phi + \lambda_\mu A_\mu S H_u H_d + \lambda_{iN^c} A_{iN^c} \Phi \tilde{N}_i^{c2} - a_S S \lambda M^2 / 2 + \text{h.c.} \right) + m_\alpha^2 |X^\alpha|^2, \quad (4.4)$$

where  $m_\alpha, A_\lambda, A_\mu, A_{iN^c}$  and  $a_S$  are soft SUSY breaking mass parameters. Rotating  $S$  in the real axis by an appropriate  $R$ -transformation, choosing conveniently the phases of  $A_\lambda$  and  $a_S$  so as the potential in Eq. (4.1) to be minimized – see Eq. (4.2c) – and substituting in  $V_{\text{soft}}$   $\langle \Phi \rangle$  and  $\langle \bar{\Phi} \rangle$  from Eq. (4.3) we get

$$\langle V_{\text{tot}}(S) \rangle = \lambda^2 M^2 S^2 / Np - 2\lambda a_{3/2} m_{3/2} M^2 S, \quad \text{where } a_{3/2} = (|A_\lambda| + |a_S|) / 2m_{3/2} > 0 \quad (4.5a)$$

is a parameter of order unity which parameterizes our ignorance for the dependence of  $|A_\lambda|$  and  $|a_S|$  on  $m_{3/2}$  and we take into account that  $m_S \ll M$ . The minimization condition for the total potential in Eq. (4.5a) w.r.t  $S$  leads to a non vanishing  $\langle S \rangle$  as follows

$$\frac{d}{dS} \langle V_{\text{tot}}(S) \rangle = 0 \quad \Rightarrow \quad \langle S \rangle \simeq 2Np a_{3/2} m_{3/2} / \lambda. \quad (4.5b)$$

The generated  $\mu$  term from the third term in Eq. (2.2b) is

$$\mu = \lambda_\mu \langle S \rangle \simeq 2\lambda_\mu Np a_{3/2} m_{3/2} / \lambda. \quad (4.6)$$

It can be comparable to  $m_{3/2}$  for  $p$  and  $N$  of order unity, if  $\lambda_\mu$  is of the same order of magnitude with  $\lambda$ . Since  $\lambda \sim 10^{-6}$ , as inferred by Eq. (3.15), the required  $\lambda_\mu$  can become compatible with Eq. (3.10) assuring, thereby, the stability of the path in Eq. (3.4) during pHI.

## 4.2 BARYOGENESIS, $\tilde{G}$ ABUNDANCE AND NEUTRINO MASSES

When pHI is over, the inflaton continues to roll down towards the SUSY vacuum, Eq. (4.3). Soon after, it settles into a phase of damped oscillations around the minimum of  $V_{\text{pHI}}$ . The (canonically normalized) inflaton,

$$\widehat{\delta\phi} = \langle J \rangle \delta\phi \quad \text{with } \delta\phi = \phi - M \quad \text{and } \langle J \rangle \simeq \sqrt{2Np} \quad (4.7)$$

acquires mass, at the SUSY vacuum in Eq. (4.3), which is given by

$$\widehat{m}_{\delta\phi} = \left\langle V_{\text{pHI}, \widehat{\delta\phi}} \right\rangle^{1/2} = \left\langle V_{\text{pHI}, \phi\phi} / J^2 \right\rangle^{1/2} \simeq \lambda M / \sqrt{Np} \quad (4.8)$$

and lies in the intermediate energy scale. E.g., for  $p = 2$  we find

$$0.14 \lesssim \widehat{m}_{\delta\phi} / \text{ZeV} \lesssim 3.8 \quad \text{with } 8 \gtrsim N \gtrsim 0.1. \quad (4.9)$$

Obviously  $\widehat{m}_{\delta\phi}$  increases as  $N$  decreases. Recall that  $1 \text{ ZeV} = 10^{12} \text{ GeV}$ .

During the phase of its oscillations at the SUSY vacuum,  $\widehat{\delta\phi}$  decays perturbatively reheating the Universe at a reheat temperature given by [5]

$$T_{\text{rh}} = \left( \frac{40}{\pi^2 g_{\text{rh}*}} \right)^{1/4} \left( \widehat{\Gamma}_{\delta\phi} m_{\text{P}} \right)^{1/2} \quad \text{with} \quad \widehat{\Gamma}_{\delta\phi} = \widehat{\Gamma}_{\delta\phi \rightarrow N_i^c N_i^c} + \widehat{\Gamma}_{\delta\phi \rightarrow H_u H_d}. \quad (4.10)$$

Also  $g_* = 228.75$  counts the MSSM effective number of relativistic degrees of freedom. To compute  $T_{\text{rh}}$  we take into account the following decay widths:

$$\widehat{\Gamma}_{\delta\phi \rightarrow N_i^c N_i^c} = \frac{g_{iN^c}^2 \widehat{m}_{\delta\phi}}{16\pi} \left( 1 - \frac{4M_{iN^c}^2}{\widehat{m}_{\delta\phi}^2} \right)^{3/2} \quad \text{with} \quad g_{iN^c} = \sqrt{2} \lambda_{iN^c} / \langle J \rangle, \quad (4.11a)$$

$$\widehat{\Gamma}_{\delta\phi \rightarrow H_u H_d} = \frac{2}{8\pi} g_H^2 \widehat{m}_{\delta\phi} \quad \text{with} \quad g_H = \lambda_\mu / \sqrt{2} \quad (4.11b)$$

which arise from the lagrangian terms

$$\mathcal{L}_{\widehat{\delta\phi} \rightarrow N_i^c N_i^c} = -\frac{1}{2} e^{K/2m_{\text{P}}^2} W_{B, N_i^c N_i^c} N_i^c N_i^c + \text{h.c.} = g_{iN^c} \widehat{\delta\phi} (N_i^c N_i^c + \text{h.c.}) + \dots, \quad (4.12a)$$

$$\mathcal{L}_{\widehat{\delta\phi} \rightarrow H_u H_d} = -e^{K/m_{\text{P}}^2} K^{SS^*} |W_{B,S}|^2 = -g_H \widehat{m}_{\delta\phi} \widehat{\delta\phi} (H_u^* H_d^* + \text{h.c.}) + \dots \quad (4.12b)$$

describing  $\widehat{\delta\phi}$  decay into a pair of  $N_j^c$  and  $H_u$  and  $H_d$  respectively. Note that  $N_j^c$  acquire masses  $M_{jN^c} = \sqrt{2} \lambda_{jN^c} M$  and we work in the so-called  $N_i^c$ -basis, where  $M_{jN^c}$  is diagonal, real and positive.

For  $T_{\text{rh}} < M_{iN^c}$ , the out-of-equilibrium decay of  $N_i^c$  generates a lepton-number asymmetry (per  $N_i^c$  decay),  $\varepsilon_i$ . The resulting lepton-number asymmetry is partially converted through sphaleron effects into a yield of the observed BAU [5]

$$Y_B = -0.35 \cdot \frac{3}{2} \frac{T_{\text{rh}}}{\widehat{m}_{\delta\phi}} \sum_i \frac{\widehat{\Gamma}_{\delta\phi \rightarrow N_i^c N_i^c}}{\widehat{\Gamma}_{\delta\phi}} \varepsilon_i, \quad (4.13)$$

where  $\varepsilon_i$  are calculated as analyzed in Ref. [9]. The expression above has to match with the observational value [6]

$$Y_B = (8.75 \pm 0.085) \cdot 10^{-11}. \quad (4.14)$$

The validity of Eq. (4.13) requires that the  $\widehat{\delta\phi}$  decay into a pair of  $N_i^c$ 's is kinematically allowed for at least one species of the  $N_i^c$ 's and also that there is no erasure of the produced  $Y_L$  due to  $N_1^c$  mediated inverse decays and  $\Delta L = 1$  scatterings. These prerequisites are ensured if we impose

$$10T_{\text{rh}} \lesssim M_{1N^c} \lesssim \widehat{m}_{\delta\phi}/2. \quad (4.15)$$

The quantity  $\varepsilon_i$  can be expressed in terms of the Dirac masses of  $\nu_i$ ,  $m_{iD}$ , arising from the third term of  $W$  in Eq. (2.2b). Employing the seesaw formula we can then obtain the light-neutrino mass matrix  $m_\nu$  in terms of  $m_{iD}$  and  $M_{iN^c}$ . As a consequence, nTL can be nicely linked to low energy neutrino data [14].

The required  $T_{\text{rh}}$  in Eq. (4.13) must be compatible with constraints on the gravitino ( $\widetilde{G}$ ) abundance,  $Y_{3/2}$ , at the onset of *nucleosynthesis* (BBN), which is estimated to be [13]

$$Y_{3/2} \simeq 1.9 \cdot 10^{-13} T_{\text{rh}}/\text{EeV}, \quad (4.16)$$

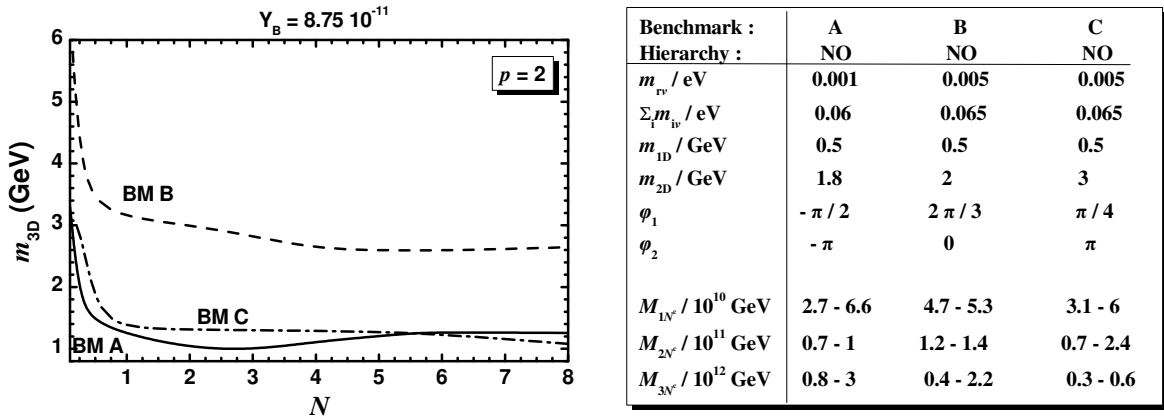


**FIGURE 3:** Contours in the  $N - m_{3D}$  plane yielding the central  $Y_B$  in Eq. (4.14) consistently with the remaining inflationary and post-inflationary requirements for  $m_{3/2} = 10\mu = 50 \text{ TeV}$ ,  $N_{\text{st}} = 1$  and the values of  $m_{i\nu}$ ,  $m_{1D}$ ,  $m_{2D}$ ,  $\varphi_1$  and  $\varphi_2$  which correspond to benchmarks A (solid line), B (dashed line) and C (dot-dashed line) shown in the Table.

where we take into account only thermal production of  $\tilde{G}$ , and assume that  $\tilde{G}$  is much heavier than the MSSM gauginos. Avoidance any disturbance to BBN entails [13]

$$Y_{3/2} \lesssim \begin{cases} 10^{-14} \\ 10^{-13} \end{cases} \quad \text{for } m_{3/2} \simeq \begin{cases} 0.69 \text{ TeV} \\ 10.6 \text{ TeV} \end{cases} \quad \text{implying } T_{\text{rh}} \lesssim 5.3 \cdot \begin{cases} 0.01 \text{ EeV} \\ 0.1 \text{ EeV} \end{cases}, \quad (4.17)$$

for the typical case where  $\tilde{G}$  decays with a tiny hadronic branching ratio. The bounds above can be somehow relaxed in the case of a short or very short-lived  $\tilde{G}$  – cf., e.g., Ref. [15].

### 4.3 RESULTS

Confronting with observations  $Y_B$  and  $Y_{3/2}$  – see Eqs. (4.14) and (4.17) – which depend on  $\hat{m}_{\delta\phi}$ ,  $T_{\text{rh}}$ ,  $M_{iNc}$  and  $m_{iD}$ 's – see Eqs. (4.13) and (4.16) – we can further constrain the parameter space of the our model. We follow the bottom-up approach detailed in Ref. [9], according to which we find the  $M_{iNc}$ 's by using as inputs the  $m_{iD}$ 's,  $m_{1\nu}$  for *normal ordered* (NO) *neutrino masses*  $m_{i\nu}$ 's, the two Majorana phases  $\varphi_1$  and  $\varphi_2$  of the PMNS matrix, and the best-fit values for the remaining neutrino oscillation parameters. Namely, we take as inputs the recently updated best-fit values [14] – cf. Ref. [9] – on the neutrino oscillation parameters including IceCube IC24 with Super Kamiokande (SK) atmospheric data. We consider only the scheme of NO  $m_{i\nu}$ 's, which can become consistent with the upper bound on the sum of  $m_{i\nu}$ 's

$$\sum_i m_{i\nu} \leq 0.082 \text{ eV}, \quad (4.18)$$

induced from P-ACT-LB data [6] at 95% c.l. Namely, we take [14]  $\Delta m_{21}^2 = 7.49 \cdot 10^{-5} \text{ eV}^2$  and  $\Delta m_{31}^2 = 2.513 \cdot 10^{-3} \text{ eV}^2$  for the mass-squared differences,  $\sin^2 \theta_{12} = 0.308$ ,  $\sin^2 \theta_{13} = 0.02215$  and  $\sin^2 \theta_{23} = 0.47$  for the mixing angles, and  $\delta = 1.1788\pi$  for the CP-violating Dirac phase.

Some representative results of our analysis are presented in Fig. 3 where we depict curves in the  $N - m_{3D}$  plane which yield the central  $Y_B$  in Eq. (4.14) for  $p = 2$ ,  $\mu = 0.1m_{3/2} = 5 \text{ TeV}$  and

$N_{\text{st}} = 1$  consistently with Eq. (3.17) – (3.19) and Eq. (4.17) – note that the allowed  $N$  values are given in Eq. (4.9). We use solid, dashed and dot-dashed line when the remaining inputs – i.e.  $m_{1\nu}$ ,  $m_{1D}$ ,  $m_{2D}$ ,  $\varphi_1$ , and  $\varphi_2$  – correspond, respectively, to benchmarks A, B and C of the Table in Fig. 3. Since the range of  $Y_B$  in Eq. (4.14) is very narrow, the 95% c.l. width of these contours is negligible. The gauge symmetry considered in work does not predict any particular Yukawa unification pattern and so, the  $m_{iD}$ 's are free parameters. This fact facilitates the fulfilment of the bounds in Eq. (4.15) since  $m_{1D}$  affects heavily  $M_{1N^c}$ . Care is also taken so that the perturbativity of  $\lambda_{iN^c}$  holds, i.e.,  $\lambda_{iN^c}^2/4\pi \leq 1$ . In all cases the inflaton  $\widehat{\delta\phi}$  decays into  $N_i^c$ 's with  $i = 1$  and  $2$  with  $\widehat{\Gamma}_{\delta\phi \rightarrow N_i^c N_i^c} > \widehat{\Gamma}_{\delta\phi \rightarrow H_u H_d}$  and so the ratios  $\widehat{\Gamma}_{\delta\phi \rightarrow N_i^c N_i^c}/\widehat{\Gamma}_{\delta\phi}$  do not introduce a considerable reduction in the derivation of  $Y_B$ . As we observe from the data in Fig. 3, successful nTL requires  $M_{iN^c}$  and  $m_{3D}$  in the ranges (0.01 – 1) ZeV and (0.5 – 6) GeV respectively. As regards the other quantities, in all we obtain

$$2.7 \cdot 10^{-2} \lesssim T_{\text{rh}}/\text{EeV} \lesssim 3 \quad \text{with} \quad 0.3 \lesssim \lambda_\mu/10^{-6} \lesssim 9.4, \quad (4.19)$$

where the variation of  $\lambda_\mu$  is explained due to the variation of  $N$  – see Eq. (4.6). Although we did not study the impact of a variation of  $\mu/m_{3/2}$  to our results, we intuitively expect that increasing  $\mu/m_{3/2}$  beyond its present value 0.1 makes the achievement of the correct  $Y_B$  and  $Y_{3/2}$  difficult. This is because an increase of  $\mu/m_{3/2}$  implies an elevation of  $\lambda_\mu$  – see Eq. (4.6) – and of  $\widehat{\Gamma}_{\delta\phi \rightarrow H_u H_d}$  in Eq. (4.11b). The last effect causes a reduction of the ratio  $\widehat{\Gamma}_{\delta\phi \rightarrow N_i^c N_i^c}/\widehat{\Gamma}_{\delta\phi}$  which entails an increase to  $T_{\text{rh}}$  in order to readjust  $Y_B$ . However, the increase on  $T_{\text{rh}}$  increases  $Y_{3/2}$  and renders the  $\widetilde{G}$  problem more acute. Therefore, our scheme primarily prefers  $\mu/m_{3/2} \lesssim 1$  – cf. Ref. [5] – which is defended by various analysis [16–18] of MSSM.

As a bottom line, nTL not only is a realistic possibility within our setting but also it can be comfortably reconciled with the  $\widetilde{G}$  constraint even for  $m_{3/2} \sim 1$  TeV as deduced from Eqs. (4.19) and (4.17).

## 5. CONCLUSIONS

We investigated the realization of pHI and nTL in the framework of a  $B - L$  extension of MSSM endowed with the condition that the GUT scale is determined by the running of the three gauge coupling constants of MSSM. Our setup is tied to the super- and Kähler potentials given in Eqs. (2.2b) and (2.3). Prominent in this setting is the role of the inflationary part of  $K$ ,  $\widetilde{K}_I$ , in Eq. (2.4b) which is rational and exhibits a shift symmetry which making it to vanish during pHI. Its free parameters ( $p, N$ ) can be constrained by the observations – see e.g. Eq. (3.21). Despite  $\widetilde{K}_I$  does not enjoy a specific symmetry as in the case of T-model HI [2,3], it assists in obtaining an excellent match with P-ACT-LB-BK18 data – see Fig. 2. In addition, our model exhibits the following features: (i) It assures possibly detectable primordial gravitational waves for natural (of order unity) ( $p, N$ ) values; (ii) It inflates away cosmological defects; (iii) It offers a nice solution to the  $\mu$  problem of MSSM, provided that  $\lambda_\mu$  in Eq. (2.2b) is somehow small; (iv) It allows for baryogenesis via nTL compatible with  $\widetilde{G}$  constraint and neutrino data. In particular, we may have  $m_{3/2} \sim 1$  TeV, with the inflaton decaying mainly to  $N_1^c$  and  $N_2^c$  – we obtain  $M_{iN^c}$  in the range ( $10^{10} - 10^{12}$ ) GeV. It remains to introduce a consistent soft SUSY-breaking sector to gain a more precise completion.

## REFERENCES

- [1] R. Kallosh and A. Linde, *Universality Class in Conformal Inflation*, *J. Cosmol. Astropart. Phys.* **07**, 002 (2013) [[arXiv:1306.5220](#)].
- [2] C. Pallis, *T-Model Higgs Inflation in Supergravity*, *J. Cosmol. Astropart. Phys.* **05**, 043 (2021) [[arXiv:2307.14652](#)].
- [3] C. Pallis, *T-Model Higgs Inflation in Supergravity*, *HEP23*, 73 [[arXiv:2307.14652](#)].
- [4] C. Pallis, *ACT-Inspired Kähler-Based Inflationary Attractors*, *J. Cosmol. Astropart. Phys.* **09**, 061 (2025) [[arXiv:2507.02219](#)].
- [5] C. Pallis, *Updating GUT-Scale Pole Higgs Inflation After ACT DR6*, *Phys. Rev. D* **113**, no. 1, 015033 (2026) [[arXiv:2510.02083](#)].
- [6] T. Louis *et al.* [ACT Collaboration], *The Atacama Cosmology Telescope: DR6 Power Spectra, Likelihoods and  $\Lambda$ CDM Parameters*, *J. Cosmol. Astropart. Phys.* **11**, 062 (2025) [[arXiv:2503.14452](#)].
- [7] E. Calabrese *et al.* [ACT Collaboration], *The Atacama Cosmology Telescope: DR6 Constraints on Extended Cosmological Models*, *J. Cosmol. Astropart. Phys.* **11**, 063 (2025) [[arXiv:2503.14454](#)].
- [8] R. Kallosh and A. Linde, *On the Present Status of Inflationary Cosmology*, *Gen. Rel. Grav.* **57**, no. 10, 135 (2025) [[arXiv:2505.13646](#)].
- [9] C. Pallis, *Gravitational Waves,  $\mu$  Term  $\mathcal{E}$  Leptogenesis from  $B - L$  Higgs Inflation in Supergravity*, *Universe* **4**, no. 1, 13 (2018) [[arXiv:1710.05759](#)].
- [10] P. Creminelli *et al.* *Detecting Primordial B-Modes after Planck*, *J. Cosmol. Astropart. Phys.* **11**, 031 (2015) [[arXiv:1502.01983](#)].
- [11] C. Pallis and N. Toumbas, *Starobinsky-Type Inflation With Products of Kähler Manifolds*, *J. Cosmol. Astropart. Phys.* **05**, no. 05, 015 (2016) [[arXiv:1512.05657](#)].
- [12] G. Lazarides and C. Pallis, *Shift Symmetry and Higgs Inflation in Supergravity with Observable Gravitational Waves*, *J. High Energy Phys.* **11**, 114 (2015) [[arXiv:1508.06682](#)].
- [13] M. Kawasaki, K. Kohri, T. Moroi and Y. Takaesu, *Revisiting Big-Bang Nucleosynthesis Constraints on Long-Lived Decaying Particles*, *Phys. Rev. D* **97**, no. 2, 023502 (2018) [[arXiv:1709.01211](#)].
- [14] I. Esteban, M.C. Gonzalez-Garcia, M. Maltoni, I. Martinez-Soler, J.P. Pinheiro and T. Schwetz, *NuFit-6.0: updated global analysis of three-flavor neutrino oscillations*, *JHEP* **12**, 216 (2024) [[arXiv:2410.05380](#)].
- [15] C. Pallis, *Induced-Gravity Higgs Inflation in Palatini Supergravity Confronts ACT DR6*, [arXiv:2602.05623](#).
- [16] N. Karagiannakis, G. Lazarides and C. Pallis, *Probing the hyperbolic branch/focus point region of the constrained minimal supersymmetric standard model with generalized Yukawa quasiunification*, *Phys. Rev. D* **92**, no.8, 085018 (2015) [[arXiv:1503.06186](#)].
- [17] P. Athron *et al.* [GAMBIT], *Global fits of GUT-scale SUSY models with GAMBIT*, *Eur. Phys. J. C* **77**, no.12, 824 (2017) [[arXiv:1705.07935](#)].
- [18] I. Khan, A. Muhammad, T. Li and S. Raza, *Revisiting the Electroweak Supersymmetry from the Generalized Minimal Supergravity*, [arXiv:2506.18442](#).